Food Chemistry 463 (2025) 141208

Contents lists available at ScienceDirect

Food Chemistry

journal homepage: www.elsevier.com/locate/foodchem

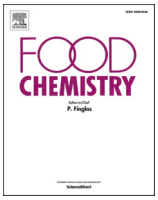

Unlocking the *in vitro* neuroprotection of sloe residues phenolic extracts by bioanalytical and chemometric strategies

Esther Gómez-Mejía [a,*,1], David Vicente-Zurdo [a,b,**,1], Noelia Rosales-Conrado [a], María Eugenia León-González [a]

[a] Department of Analytical Chemistry, Faculty of Chemistry Sciences, Complutense University of Madrid, 28040 Madrid, Spain
[b] Centre for Metabolomics and Bioanalysis (CEMBIO), Department of Chemistry and Biochemistry, Faculty of Pharmacy, San Pablo-CEU Universities, CEU Universities, 28660, Boadilla Del Monte, Madrid, Spain

ARTICLE INFO

Keywords:
Sloe bio-residues
Circular economy
Polyphenols
Alzheimer's disease
In vitro antioxidant
$A\beta_{42}$
Chemometric tools

ABSTRACT

Wild fruits, particularly the underutilized sloe (*Prunus spinosa*), are gaining interest as natural antioxidants, with residues from liqueur production being a source of bioactive compounds. This study proposes a sustainable approach for valorizing sloe residues, seeds and skins, by employing an innovative green extraction method. HPLC-ESI-QTOF and spectrophotometric techniques were used to explore the phenolic profile, highlighting the predominance of quercetin, 2,3-dihydroxybenzoic and ferulic acids (9.7–57 $\mu g \cdot g^{-1}$). In addition, the presence of Cu, Zn and Ca was confirmed by atomic absorption spectroscopy. Simultaneously, their neuroprotective potential against Alzheimer's disease (AD) was studied by exploring the inhibition of beta-amyloid aggregation and oxidative stress cytoprotection in SH-SY5Y cell line, standing out 1 $\mu g \cdot g^{-1}$ and 10 $\mu g \cdot g^{-1}$ extracts of sloe skin. Phenolic composition was correlated with bioactivities by means of multivariate analysis. These results contributed to highlight the potential of this bio-residue as a neuroprotective agent against AD in pharmaceutical and nutraceutical industries.

1. Introduction

The growing interest in wild fruits as new natural antioxidants, particularly those of the genus *Prunus*, has opened new avenues for the exploration of their potential health benefits and industrial applications (Opriş et al., 2021; Popović et al., 2020). Among them, the fruits of *Prunus spinosa* L. or sloe berries, produced by blackthorn tree native to Europe, West Asia and North Africa (Sabatini et al., 2020), are replete of various bioactive constituents such as polyphenols, anthocyanins, ascorbic acid, carbohydrates, macro- and microminerals (Negrean et al., 2023). Of particular interest are polyphenols, a varied array of phytochemicals, widely recognized as potent antioxidants related to the prevention and onset of pathological conditions, including cancer, diabetes, and neurodegenerative disorders such as Alzheimer's disease (AD) (Silva & Pogačnik, 2020).

Sloe berries are traditionally consumed raw or used in the preparation of jams, teas and liquor-based beverages such as *Pacharán* (northern Spain). As a result, spent sloe berries, seeds and stems processing bio-residues are generated, which has a direct deleterious impact on local agro-industrial environments (Barros et al., 2016; Farag et al., 2022). These sloe wastes might serve as a bountiful and underexploited source of bioactive polyphenols with significant added value (Negrean et al., 2023).

Such valorization of sloe residues aligns seamlessly with the principles of Circular Economy and Green Chemistry (Barros et al., 2016; Capaldi et al., 2024), still also necessitating adherence to the approach

Abbreviations: ACN, acetonitrile; AD, Alzheimer's disease; ANOVA, analysis of variance; Aβ42, beta-amyloid; ESI, electrospray ionization; FA, formic acid; FAAS, flame atomic absorption spectroscopy; GAE, gallic acid equivalent; HFIP, 1,1,1,3,3,3-hexafluoro-2-propanol; HPLC, high-performance liquid chromatography; LOD, limit of detection; LOQ, limits of quantification; MSPD, matrix solid-phase dispersion; MTT, 3-(4,5-dimethylthiazol-2-yl)-2,5-diphenyltetrazolium bromide; PBS, phosphate-buffered saline; PCA, principal component analysis; QE, quercetin equivalent; SD, standard deviation; SH-SY5Y, human neuroblastoma cells; SLE, solid-liquid extraction; TEM, transmission electron microscopy; TFC, total flavonoid content; TPC, total phenolic content.

* Corresponding author.
** Corresponding author at: Department of Analytical Chemistry, Faculty of Chemistry Sciences, Complutense University of Madrid, 28040 Madrid, Spain.
E-mail addresses: egomez03@ucm.es (E. Gómez-Mejía), davidvic@ucm.es (D. Vicente-Zurdo).
[1] Authors with equal contribution.

https://doi.org/10.1016/j.foodchem.2024.141208
Received 12 July 2024; Received in revised form 5 September 2024; Accepted 7 September 2024
Available online 10 September 2024

of Green Extraction, that is, sustainable extraction methodologies that are time and energy efficient, reduce the use of organic solvents, and optimally valorize natural resources (Capaldi et al., 2024). Accordingly, matrix solid-phase dispersion (MSPD) stands out as innovative, inexpensive, green extraction technique that integrates sample preparation and extraction in a single step (Wianowska & Gil, 2019). This technique requires minimal instrumentation and emerges as a versatile technique suitable for both small- and large-scale applications. Additionally, MSPD operates under ambient conditions, *i.e.*, room temperature and atmospheric pressure, which guarantees the preservation of the functional properties of the extract for future applications (Castillo et al., 2022).

This technique has been previously employed for the extraction of polyphenols from other horticultural bio-residues (Castillo et al., 2022; Du et al., 2018; Gómez-Mejía et al., 2019; Gómez-Mejía, Vicente-Zurdo, et al., 2022). Although studies have been conducted on the polyphenol profile in sloe genotypes and fruits obtained through conventional extraction methods (Magiera et al., 2022; Popović et al., 2020; Pozzo et al., 2019; Sabatini et al., 2020), comprehensive data on the remaining phenolic profile of sloe bio-residues remain largely unexplored, particularly those derived from green chemistry and green extraction, underscoring the unprecedented nature of the application of MSPD for the recovery and study of phenolic compounds from *P. spinosa* residues.

Along these lines, research on the bioactive response of *P. spinosa* fruits has focused mainly on their antioxidant, antidiabetic, antimicrobial, anti-inflammatory and anticarcinogenic activity (Magiera et al., 2022; Negrean et al., 2023; Opriş et al., 2021; Popović et al., 2020; Pozzo et al., 2019; Sabatini et al., 2020). Be that as it may, no research has been conducted concerning the neuroprotective potential of phenolic extracts from *P. spinosa*, either in sloe fruits or bio-residues, in the context of neurodegenerative disorders such as AD. This condition is the most prevalent, accounting for 80 % of all dementia cases worldwide (Chen et al., 2023). Currently, it lacks effective treatments, resulting in significant socioeconomic costs. Therefore, the search for potential neuroprotective agents to prevent the onset and progression of these diseases remains a major challenge (Moyano et al., 2021).

According to the "Amyloid Cascade Hypothesis", the pathogenesis of AD is largely attributed to the accumulation and aggregation of beta-amyloid ($A\beta_{42}$) protein, which forms insoluble plaques associated with neuronal dysfunction and cell death, being therefore the origin of this disease (Karran & De Strooper, 2016; Mezeiova et al., 2019). In addition, the role of metal ions, in particular iron, copper, and zinc, in exacerbating AD pathology through their interaction with $A\beta_{42}$ and contribution to neuronal oxidative stress through Fenton reaction has also been (Chen et al., 2023). Therefore, a crucial aspect in research against neurodegenerative diseases revolves around evaluating the antioxidant and anti-amyloidogenic properties of the study compounds, as well as their interaction with the aforementioned metals.

Therefore, this study uniquely explores the neuroprotective potential of phenolic extracts obtained from unexamined bio-residues of spent sloe (seeds and skins), highlighting the innovative application of MSPD-green extraction method, applying different bioanalytical tools in this context. To this end, the phenolic content was characterized by spectrophotometric and HPLC-ESI-QTOF methods, simultaneously the *in vitro* antioxidant activity was studied using the human neuroblastoma cell line SH-SY5Y and the anti-amyloidogenic effect was visualized by Transmission Electron Microscopy (TEM), for the very first time. The presence of Cu, Fe and Zn was also determined by Flame Atomic Absorption Spectroscopy (FAAS), and multivariate analysis was conducted to correlate bioactive responses with the main phenolic compounds of the residual sloe extracts.

2. Materials and methods

2.1. Reagents, standards and solvents

Analytical grade reagents and purified water from a Milli-Q system (Millipore, Bedford, MA, USA) were required in all experimental procedures performed. Absolute ethanol (EtOH), acetonitrile (ACN), methanol (MeOH) and formic acid (FA) of MS quality, as well as hydrochloric acid (HCl, 37 %), were provided by Scharlab (Barcelona, Spain). $FeCl_2$, $CuCl_2$, $ZnCl_2$ and $CaCl_2$ were purchased from Merck (Madrid, Spain). Dimethyl sulfoxide (DMSO), curcumin (> 65 %), 1,1,1,3,3,3-hexafluoro-2-propanol (HFIP) and fragment 1–42 of amyloid-β protein ($A\beta_{42}$) (A9810, CAS: 107761–42-2) were supplied by Sigma-Aldrich (St. Louis, MO, USA).

Phenolic compounds: caffeic acid (≥ 98.0 %), catechin (≥ 98.0 %), chlorogenic acid (≥ 95.0 %), *p*-coumaric acid (≥ 98.0 %), 2,3-dihydroxybenzoic acid (≥ 97.0 %), epicatechin (≥ 98.0 %), *trans*-ferulic acid (98 %), gallic acid monohydrate (≥ 98.0 %), kaempferol (≥ 97.0 %), myricetin (≥ 96.0 %), naringin (≥ 95.0 %), quercetin (≥ 95.0 %), resveratrol (≥ 99.0 %) and rutin trihydrate (≥ 95.0 %) were distributed by Sigma-Aldrich (St. Louis, MO, USA). Hesperidin (≥ 98.0 %) was provided by European Pharmacopoeia. Phenolic stock solutions were prepared in methanol, ethanol-water 80:20 (*v*/v) (quercetin) or 5 % (v/v) DMSO (hesperidin) to a final concentration of 200 $mg{\cdot}L^{-1}$; and were stored in the dark at 4 °C or at −80 °C (hesperidin, catechin, *trans*-ferulic and caffeic acids) for no longer than one month.

2.2. Biowaste material

The sloe residue samples (*P. spinosa*) were provided by Hijos de Pablo Esparza Bodegas Navarras S.A. (Navarra, Spain). The samples were obtained as biowaste in the manufacture of a commercialized sloe gin known as *Pacharán*. Precisely, a mixture of wild sloe berries from Bulgaria and cultured sloe berries from Spain, were macerated in aniseed at a controlled temperature for 6 months and then separated from the beverage by decanting. Finally, the seeds and skins of the sloes were manually separated in order to compare the different parts of the bio-residue. Then, both fractions were homogenized in a mixer mill (MM 301, Retsch) to 20 mesh and stored in air-tight opaque containers at 4 °C.

2.3. Moisture and ashes determination

Moisture content was determined following the official method of analysis AOAC 925.10 (AOAC International, 2000). Briefly, 1 g of sloe skins or seeds was weighed in triplicate to the nearest ±0.1 mg. Then, fresh samples were placed in an oven (P-Selecta, Panreac, Barcelona, Spain) at (102 ± 2) °C for a minimum of 3 h. After cooling in a desiccator for at least 20 min, the dried samples were weighted to constant mass.

Ashes were determined according to official method of analysis AOAC 923.03 (AOAC International, 2003). A total of 1 g of each of sloe bio-residue (skins and seeds) was weighted by triplicate and placed in a cold muffle furnace (Nabertherm N 14/11/P300, Bremen, Germany), heated at $2\ °C{\cdot}min^{-1}$ to 550 °C for 4 h and maintained at (550 ± 5) °C for a minimum of 3 h. Thereafter, the calcined samples were placed in a desiccator for 30 min and weighed to obtain the ash content in the sloe skin and seed.

2.4. Extraction of polyphenols by matrix solid-phase dispersion

An optimized simple and fast MSPD extraction method was carried out as previously stated by (Gómez-Mejía, Vicente-Zurdo, et al., 2022). Briefly, 0.1000 g of sloe seeds or skins and 0.0500 g of diatomaceous earth (Restek Corporation) was meticulously blended for 2 min in a porcelain mortar. Subsequently, this mixture was quantitative transferred into a plastic tube and 2 mL of an 80:20 (*v*/v) ethanol-water solution were added. Following this step, the combination was subjected to ultrasonic treatment for 5 min (ultrasound bath WX, VELP Scientifica, 720 W and 3.1 % amplitude). Finally, after a centrifugation step (centrifuge 5804, Eppendorf) lasting 25 min at 1528*g*, a clear supernatant was obtained. This entire procedure was conducted in triplicate,

and the phenolic extract was then accurately weighed for subsequent experiments.

2.5. Determination of Total phenolic content

The determination of the Total Phenolic Content (TPC) was performed following a previously described spectrophotometric method (Vijayalaxmi et al., 2015), with some adjustments. Concisely, a volume of 500–600 μL of hydroethanolic extract of sloe skin or seed was mixed with 70 μL of Folin-Ciocalteu reagent and 60 μL of a 7.5 % (v/v) aqueous solution of Na_2CO_3. Milli-Q water was then added to bring the final volume to 10 mL. The absorbance of the resulting solution was measured at 720 nm (UV–Vis Thermo Scientific Multiskan spectrophotometer, Agilent Technologies). Gallic acid standard was used for quantitative purposes (calibration curve from 0 to 60 μmol·L^{-1}, $n = 5$). The results were expressed as mg of gallic acid equivalent per g of dried sample (mg GAE·g^{-1} sample). All samples were prepared in triplicate under the various experimental conditions examined.

2.6. Determination of total flavonoid content

The aluminum complexation colorimetry method was employed for estimating the Total Flavonoid Content (TFC) (Vijayalaxmi et al., 2015). For this analysis, 2 mL of Milli-Q water were mixed with 300 to 500 μL of sloe skins or seed extract and 150 μL of a 5 % aqueous solution of $NaNO_2$. After a 5-min reaction, 150 μL of 10 % $AlCl_3$ solution was added and allowed to further react for another 5 min. Then, 1 mL of 1 M NaOH was incorporated to the solution, thoroughly mixed and allowed to stand for 15 min. Finally, Milli-Q water was added to reach a final volume of 10 mL, and the absorbance was measured at 415 nm (UV–Vis Thermo Scientific Multiskan spectrophotometer, Agilent Technologies). For quantification, quercetin served as the standard, and a calibration curve was obtained within 0–45 μmol·L^{-1} ($n = 6$). The results were expressed as mg of quercetin equivalents per g of dried extract (mg QE·g^{-1}). All samples were prepared in triplicate under the various experimental conditions investigated.

2.7. Analysis of phenolic compounds by liquid chromatography coupled to tandem mass spectrometry

The phenolic profile of the hydroethanolic extracts of sloe seeds and skins, obtained using the optimized MSPD extraction procedure, was carried out by high-performance liquid chromatography coupled to a quadrupole time-of-flight mass spectrometer (HPLC-ESI-QTOF) following a non-targeted analysis. The instrumentation consisted of an Agilent liquid chromatography system (Model 1200), with a quaternary pump (G1311A), a degasser (G1322A), an automatic injector equipped with a thermostat (G1367B), a column module also equipped with a thermostat (G1316A), and a QTOF mass spectrometer (Agilent G6530A) featuring electrospray ionization (ESI) under atmospheric pressure and JetStream technology. The latter operated in negative ionization mode and scanning mode (SCAN) over 100–1000 *m/z* range, using a capillary voltage of 4 kV and a pressure of 45 psi. Data processing was undertaken with Masshunter Data Acquisition B.05.00, Masshunter Qualitative Analysis B.07.00, and Massprofinder Professional B.08.00. Nitrogen was used as nebulising and drying gas (10.0 L·min^{-1}, 325 °C).

The HPLC-ESI-QTOF separation was performed using a Synergi™ C18 Fusion-RP 80 Å analytical column (150 mm × 3 mm I.D., 4 μm, Phenomenex, USA) maintained at 30 °C. A mobile phase gradient consisting of a combination of 0.1 % (*v*/v) FA in ACN (solvent A) and 0.1 % (v/v) aqueous FA solution (solvent B) was implemented in the following manner: initially, 10 % of solvent B was maintained for 0.1 min, then increased linearly to 35 % over 30 min, reaching 70 % in 5 min. This state was maintained for 2 min, followed by a final linear increase to 90 % B over 3 min, and sustained for 5 min. Subsequently, the gradient was re-equilibrated. The flow rate was set at 0.50 mL·min^{-1}, and the injection volume at 20 μL (Gómez-Mejía et al., 2023).

Identification of phenolic compounds was based on the acquired high-resolution mass data gather from commercial standards and/or databases (FooDB and Mass Bank). Quantification was achieved through 5-level external calibration curves (3 independent measurements) for commercially available phenolic standards. Coefficients of determination (R^2) for each polyphenol ranged from 0.9962 to 0.9998. Equations for the standards curves for each polyphenol were as follows: gallic acid, $y = (2.0 \pm 0.1) \cdot 10^7\ L{\cdot}\mu g^{-1}\ x + (1.0 \pm 0.1) \cdot 10^6$; 2,3-dyhydroxibenzoic acid, $y = (1.7 \pm 0.1) \cdot 10^7\ L{\cdot}\mu g^{-1}\ x + (1.0 \pm 0.1) \cdot 10^6$; caffeic acid, $y = (2.98 \pm 0.07) \cdot 10^7\ L{\cdot}\mu g^{-1}\ x + (8.0 \pm 0.7) \cdot 10^5$; catechin, $y = (1.61 \pm 0.01) \cdot 10^7\ L{\cdot}\mu g^{-1}\ x + (9 \pm 1) \cdot 10^4$; epicatechin, $y = (1.31 \pm 0.02) \cdot 10^7\ L{\cdot}\mu g^{-1}\ x + (2 \pm 1) \cdot 10^5$; *p*-coumaric acid, $y = (1.7 \pm 0.1) \cdot 10^7\ L{\cdot}\mu g^{-1}\ x + (8.0 \pm 0.7) \cdot 10^5$; rutin, $y = (2.23 \pm 0.02) \cdot 10^7\ L{\cdot}\mu g^{-1}\ x + (0 \pm 2) \cdot 10^5$; *trans*-ferulic acid, $y = (5.4 \pm 0.1) \cdot 10^6\ L{\cdot}\mu g^{-1}\ x + (1.0 \pm 0.1) \cdot 10^5$; quercetin, $y = (3.6 \pm 0.1) \cdot 10^7\ L{\cdot}\mu g^{-1}\ x + (3 \pm 1) \cdot 10^6$; kaempferol, $y = (3.6 \pm 0.1) \cdot 10^7\ L{\cdot}\mu g^{-1}\ x + (1.0 \pm 0.1) \cdot 10^6$; naringin, $y = (1.28 \pm 0.02) \cdot 10^7\ L{\cdot}\mu g^{-1}\ x + (2 \pm 2) \cdot 10^5$; hesperidin, $y = (1.37 \pm 0.02) \cdot 10^7\ L \cdot \mu g^{-1}\ x + (3 \pm 1) \cdot 10^5$. Whenever commercial standards were unavailable, a semi-quantitative approach was applied using the most comparable standard that was accessible. Ultimately, the results were expressed in μg per g of dry sample.

2.8. Determination of metals by flame atomic absorption spectroscopy

The composition of selected metals, namely Cu, Fe and Zn, and Ca, in the skins and seeds of the sloe biowaste, as well as in their hydroalcoholic extracts was determined by flame atomic absorption spectroscopy (FAAS, Perkin-Elmer 1100 Atomic Absorption Spectrometer, using an air-acetylene flame (2.5 ratio) at a flow rate of 4.0 mL·min^{-1}), after acidic digestion of the samples in a CEM 1000 W MSP microwave oven (Stallings, NC), equipped with temperature and pressure feedback controllers and 12 high-pressure vessels (100 mL), which operated at a maximum power of 1600 W.

For this purpose, 1 g of homogenized sloe samples or extracts was weight in triplicate in digestion tubes, where 5 mL of 60 % HNO_3, 1 mL of 33 % H_2O_2, and 1 mL of Milli-Q water were added. Then the mixture was submitted to a microwave heating program comprising a 20-min ramp up to 130 °C, followed by a 10-min holding time, ensuring complete breakdown of organic materials, and facilitating accurate metal determination. Digestion blanks were prepared in parallel. Once cooled to room temperature, the resulting digests were suitably diluted to a final volume of 10 mL with Milli-Q water and filtered through a 0.22-μm Nylon filter (Scharlab, Barcelona, Spain), prior analysis (Vicente-Zurdo et al., 2019). Subsequently, FAAS was employed for metal analysis. The wavelengths employed for quantification purposes were 420.4 nm for Ca, 324.8 nm for Cu, 248.3 nm for Fe, and 213.9 nm for Zn. Calibration curves from 0.1 to 2.5 mg·L^{-1} ($n = 5$, 3 replicates) for each element were prepared daily by appropriate dilution of stock metal solutions (100 mg·L^{-1}), prepared in water acidified with HNO_3 50 % (*v*/v). Finally, the limits of detection (LODs) and limits of quantification (LOQs) were calculated as 3.3 SD/S and 10 SD/S, respectively. The standard deviation (SD) was stablished by measuring ten times the absorbance of the digestion blank. The S coefficient represents the slope of the calibration curve.

2.9. Evaluation of in vitro antioxidant activity

Human neuroblastoma cells (SH-SY5Y, CRL-2266) were procured from the ATCC and stored in a mixture comprising 90 % fetal bovine serum (FBS, ThermoFisher Scientific, Madrid, Spain) and 10 % DMSO at −130 °C in liquid nitrogen vapor until required. These SH-SY5Y cells were maintained at 37 °C in a 5 % CO_2 environment using Dulbecco's Modified Eagle Medium/Nutrient Mixture F-12 (DMEM/F12, ThermoFisher Scientific, Madrid, Spain), which was supplemented with 1 % penicillin/streptomycin and 10 % FBS. For subculture, phosphate-

buffered saline (PBS, ThermoFisher Scientific, Madrid, Spain) at pH 7.4 and trypsin-EDTA (0.05 %, ThermoFisher Scientific, Madrid, Spain) were employed. Additionally, the cells were routinely screened for mycoplasma infection using the Look Out Mycoplasma PCR Detection Kit (Sigma-Aldrich, Madrid, Spain) to ensure their integrity.

To evaluate the cytotoxicity and neuroprotective properties of skins and seed extracts against H_2O_2 injury on the SH-SY5Y cell line, 3-(4,5-Dimethylthiazol-2-yl)-2,5-diphenyltetrazolium bromide (MTT, Sigma-Aldrich, Madrid, Spain) assay was employed. Cells were seeded in 96-well plates at a density of $2.4{\cdot}10^3$ cells·well^{-1}, except for the negative controls, which contained only culture medium without cells. After 24 h, the culture medium was aspirated, and cells were exposed to 7 non-cytotoxic concentrations (ranging from 0.001 μg·L^{-1} to 1 mg·L^{-1}) of sloe for 48 h in presence and absence of 600 μM H_2O_2, except for the positive and negative controls, to which an equivalent volume of culture medium was added. Subsequently, 20 μL of a 5 mg·mL^{-1} MTT solution in PBS was added to each well, followed by incubation at 37 °C for 4 h. Afterward, culture medium was removed, and 100 μL of DMSO was added to dissolve the formazan crystals. Absorbance was measured at 570 nm, recorded after 15 min of incubation at room temperature, using a microplate spectrophotometer (Thermo Scientific Multiskan, Agilent Technologies). Cell viability was calculated using the following equation:

$$\textit{Viability}\ (\%) = \frac{A_S - A_{C^-}}{A_{C^+} - A_{C^-}} \times 100 \quad (1)$$

where A_S represents the absorbance of the sample, A_{C-} stands for the absorbance of the negative control, and A_{C+} means the absorbance of the positive control. A minimum of 5 concentration points, each with 5 replicate wells per concentration, were employed. In every experiment, both positive and negative control groups were included in parallel.

The positive controls involved untreated cells that were seeded without exposure to phenolic extracts of sloe skin or seed respectively, while the negative controls entailed measuring the culture medium in the absence of cells. Cell viability under co-incubation of H_2O_2 with skin and seed extracts was compared with co-incubation of H_2O_2 with 550 μM of Trolox to test the protection of sloe extracts against the oxidative stress induced by H_2O_2.

2.10. Study of $A\beta_{42}$ protein aggregation

The potential anti-amyloidogenic effect of phenolic extracts from sloe biowaste skins and seeds on iron-induced $A\beta_{42}$ protein aggregation, a widely related metal in neurodegenerative diseases, was evaluated by TEM.

Firstly, commercial $A\beta_{42}$ monomer was pre-treated with pure HFIP, as described by (Vicente-Zurdo et al., 2020). To achieve this, 1 mg of the frozen commercial $A\beta_{42}$ was allowed to equilibrate at room temperature for 30 min to prevent peptide condensation. Subsequently, 222 μL of HFIP was added to the peptide to create a 1 mM solution. The peptide solution was then vigorously vortexed, and 10 μL aliquots were extracted. All aliquots were subjected to a 30 min vacuum evaporation process (Savant SpeedVac, SPD121P-115, Thermo Fisher,Waltham, MA, USA) at 45 °C to eliminate any residual HFIP. Ultimately, the pretreated solid $A\beta_{42}$ monomer was stored in Eppendorf vials and frozen at −20 °C until required. Following, the pre-treated $A\beta_{42}$ monomer was allowed to equilibrate at room temperature for 10 min, and then the appropriate volume of DMSO and, subsequently, 10 mM HCl was added, sonicating the sample for 10 min after the addition of each solvent. As such an $A\beta_{42}$ stock solution of 200 μM with 4 % (*v*/v) DMSO was obtained.

Then, working solutions tested in the aggregation experiments were daily prepared by diluting stock solutions in 10 mM HCl, including a 50 μM $A\beta_{42}$ control, a 50 μM $A\beta_{42}$ plus 50 μM Fe(II) positive control, and those solutions consisting of 50 μM $A\beta_{42}$ together with 1 μg·L^{-1} sloe phenolic extract (skins or seeds) in the absence or in the presence of 50 μM Fe(II). Additionally, curcumin 50 μM was employed as a negative control. Finally, all working solutions were incubated at 37 °C for 48 h and subsequently subjected to TEM analysis. Three independent experiments were performed in duplicate.

To this end, 10 μL of each incubated working solution was placed on a carbon-coated copper grid for 5 min. Subsequently, each grid was stained with 10 μL of 1.5 % (*w*/*v*) phosphotungstic acid for another 5 min, resulting in negative staining of $A\beta_{42}$ fibrils. After removing excess staining solution, the prepared grids were transferred and examined using a JEOL JEM 1400 Plus transmission electron microscope operating at 120 kV. TEM images were captured at magnification powers of ×12,000, ×6000, and ×1000. A comparative analysis was performed to observe differences in the modulation of $A\beta_{42}$ aggregation, as well as in the width and length of fibrils, among the micrographs obtained from the protein alone and from the presence of metal, the target sloe extracts, or both. Fibril measurements were conducted using the ImageJ program ($n = 200$).

2.11. Statistical analysis

The chemical composition and neuroprotective activity data of both fractions of sloe bio-residues were statistically explored and compared by two-paired *t*-Student analysis, one-way analysis of variance (ANOVA) and the Duncan multiple comparison test, where appropriate, in addition to correlating the above it proved useful to resort to a Principal Component Analysis (PCA), using *Statgraphics 19* program (Statgraphics Technologies. Inc., Rockville, MD, USA).

3. Results and discussion

3.1. Moisture and ash determination

Analyzing moisture and ash content in sloe bio-residues, intended for valorization as functional ingredients, is of paramount importance, since it facilitates accurate assessment of nutritional composition, quality control and industrial applicability.

Moisture levels are a key indicator of the presence of water, which influences nutrient and non-nutrient concentrations, and practical issues such as manageability, transportability and storage of biowaste. Overall, the subsequent feasibility and viability of utilizing sloe bio-residues as a source of neuroprotective phenolic compounds is shaped by such parameter. Table 1 reports the moisture content of residual sloe skin and seeds. According to two-paired *t*-Student test, notable disparities were observed (p-value <0.001), with residual sloe skins showing a moisture content thirty-fold higher than sloe seeds (Table 1). Other studies have reported moisture yields between 18 % and 35 %, in sloe fruits (Babalau-Fuss et al., 2018; Damar & Yilmaz, 2023) than those described both for skins and seeds herein, suggesting the higher viability of *P. spinosa* residual seeds and skins to be valorized for food applications and functional foods on an industrial scale (Farag et al., 2022).

Regarding ash content, this parameter reflects the presence of inorganic materials in the agri-food samples, thus serving as an indicator of the concentration of minerals, such as Fe, Ca, Mg or Cu (Velickovic et al., 2016). These findings provide valuable information on the distinctive characteristics of sloe skins and seeds, shedding light on their nutritional composition and potential applications in various food-related contexts (Farag et al., 2022; Velickovic et al., 2016). The results on the ash content of sloe seeds and skins are shown in Table 1, whereas, in contrast to the moisture content, sloe seeds presented a statistical predominance of inorganic materials over sloe skins (p-value <0.001). In both samples the ash content was under 5 %, in agreement with other studies carried out on *P. spinosa* fruit (Damar & Yilmaz, 2023; Velickovic et al., 2016).

3.2. Metal determination

In the context of this study, accurate quantification of the levels of

Table 1
Moisture, ash and metal content of sloe skins and seeds, and their respective phenolic extracts.

Sample	Moisture (%)	Ash (%)	[Fe] ($\mu g \cdot g^{-1}$)	[Cu] ($\mu g \cdot g^{-1}$)	[Zn] ($\mu g \cdot g^{-1}$)	[Ca] ($mg \cdot g^{-1}$)
Skin	82.3 ± 0.4^{A}	2.2 ± 0.2^{A}	73 ± 3^{Aa}	11.2 ± 0.4^{Ab}	10 ± 2^{Ab}	3.4 ± 0.1^{A}
Seed	2.7 ± 0.1^{B}	3.67 ± 0.03^{B}	29.9 ± 0.6^{Bb}	7.5 ± 0.6^{Bc}	66 ± 6^{Ba}	2.10 ± 0.08^{B}
Skin extract	–	–	< LOD	< LOD	< LOD	0.102 ± 0.003^{C}
Seed extract	–	–	< LOD	4.7 ± 0.6^{C}	< LOQ	< LOQ
p-value	< 0.001	< 0.001	< 0.001	< 0.05	< 0.001	< 0.05

Results expressed as the mean ± standard deviation (SD); $n = 3$. Mean values with different letters indicate significant differences between samples (capital letters) and within the same sample (small letters).
Analytical parameters of FAAS method (5 calibration points, 3 independent measurements): Fe ($y = 0.0384\ L \cdot mg^{-1}\ x$, $R^2 = 0.9999$, LOD = 2 $\mu g \cdot g^{-1}$, LOQ = 8 $\mu g \cdot g^{-1}$); Cu ($y = 0.0639\ L \cdot mg^{-1}\ x + 0.021$, $R^2 = 0.9998$, LOD = 1 $\mu g \cdot g^{-1}$, LOQ = 2 $\mu g \cdot g^{-1}$); Zn ($y = 0.1911\ L \cdot mg^{-1}\ x + 0.0094$, $R^2 = 1.000$, LOD = 1 $\mu g \cdot g^{-1}$, LOQ = 4 $\mu g \cdot g^{-1}$); Ca ($y = 0.0248\ L \cdot mg^{-1}\ x$, $R^2 = 0.9993$, LOD = 2 $\mu g \cdot g^{-1}$, LOQ = 7 $\mu g \cdot g^{-1}$).

essential metals, specifically Fe, Cu and Zn, is of utmost importance due to their potential implications in the development of AD. Accumulation of these metals within the brain has been associated with aggregation of $A\beta_{42}$ protein, a hallmark of neurodegenerative disorders (Chen et al., 2023; Karran & De Strooper, 2016). In addition, the presence of Ca was also determined, as this mineral contributes to the maintenance of bone mass and provides added value to the use of sloe residues as functional ingredients (Farag et al., 2022; Velickovic et al., 2016). Furthermore, it should be mentioned that the determination of the aforementioned was directed both to the skin and seed of the residual sloe, as well as to the phenolic extracts derived from the application of a MSPD extraction. The latter was carried out to control the content of metals with neurotoxic potential within the phenolic extract, since this would be later used for the *in vitro* neuroprotective assessment.

Detailed results of metal content are presented in Table 1. This analysis revealed significant disparities in metal concentrations, both between the different parts of the residue, according to the *t*-Student, and within the same sample, according to one-way ANOVA statistical test. By far, Ca was the major element in both samples (Table 1), occurring in higher concentrations in the sloe skins (3.4 $mg \cdot g^{-1}$), followed by the metal Fe (reported at 73 $\mu g \cdot g^{-1}$ in the skin), and Zn in the sloe seeds (66 $\mu g \cdot g^{-1}$), which was six times higher than that observed in the skins (Table 1). Likewise, in both, Cu was the minor metal (< 12 $\mu g \cdot g^{-1}$), with no significant differences found with Zn concentration in sloe skins (Table 1). Prior, (Velickovic et al., 2016) reported contents of Fe and Ca in sloe fruits, within the same magnitude as those found herein, albeit slightly lower (15.8 $\mu g \cdot g^{-1}$ and 1.5 $mg \cdot g^{-1}$, respectively). Additionally, similarly to this study, (Damar & Yilmaz, 2023) found that Cu content was two to three times lower than Zn and Fe one (around 15 $\mu g \cdot g^{-1}$). The differences in plant genotype, geographic origin and maturity stages of the fruit, as well as extraction methods and agricultural practices, could explain these variations (Farag et al., 2022).

Along these lines, the MSPD extraction process led to a reduction of metal levels in both phenolic extracts of sloe skin and seeds. Thus, only the phenolic extract of sloe seeds showed Cu, quantified in at 4.7 $\mu g \cdot g^{-1}$, albeit Zn and Ca were detected below the limit of quantification of the method (Table 1). Meanwhile, in the phenolic extracts of sloe skins, none of the metals were detected, leaving aside Ca, which showed a concentration of 102 $\mu g \cdot g^{-1}$. These findings provide valuable insights into the metal profiles of sloe skins and seeds and underscore the potential impact of the extraction process on metal contents, which may have positive implications for their neuroprotective applications.

3.3. Phenolic characterization of sloe extracts

3.3.1. Chromatographic profile

Within the *Prunus* genus, sloe and its bio-residues present an intriguing case for the study of bioactive polyphenols (Pinacho et al., 2015). Yet, these compounds are not uniformly distributed in all plant tissues, so that sloe skins and seeds may contain different phenolic profiles (Sytařová et al., 2020). Also, when valorizing this waste, it is necessary to consider that sloe seeds, also harbor cyanogenic derivatives that can be harmful in excessive amounts (Farag et al., 2022). Hence, it is crucial to investigate the distribution of polyphenols and cyanogenic derivatives within the bioactive extracts of sloe skins and seeds for the effective utilization of these bio-residues, ensuring that the resulting extracts are safe and beneficial for use as neuroprotective agents.

The phenolic profile of *P. spinosa* residue skin and seed extracts was investigated by an untargeted HPLC-ESI-MS/MS approach, according to retention time, molecular ion and fragments derived from ESI-MS/MS in positive ionization mode, using commercial standards and/or databases. Based on this, 22 phenolic compounds were identified in the form of aglycones or low molecular weight glycosides (Table 2). Altogether, ten phenolic acids were recognized, comprising hydroxybenzoic acids (1, 2, 4, 7, 9) and hydroxycinnamic acids (3, 6, 8, 11, 13). In addition, twelve different flavonoids were reported, subclassified into flavanones (18, 19), flavan-3-ols (5, 10) and flavonols (12, 14–17, 20–22), the latter being the largest in number. Complementarly, FooDB database was used to identify amygdalin in both sloe extracts, failing to unequivocally confirm its presence, which highlights the potential applicability of these sloe extracts. Among the *Prunus* genus, plum, apricot and peach seeds stand out for their notable amygdalin content (Farag et al., 2022). In turn, while (Kumarasamy et al., 2003) identified, but not quantified, amygdalin, prunasin and sambunigrin in a methanolic fraction of sloe seeds, (Pinacho et al., 2015; Popović et al., 2020; Sabatini et al., 2020) neither reported the latter, nor other cyanogenic glycosides in hydroethanolic extracts of sloe fruits, which could be due to both the fruit variety and the extraction method used.

Following, the phenolic composition of the residual extracts of sloe seeds and skin, after MSPD hydroalcoholic extraction, was determined by HPLC-ESI-QTOF, and by spectrophotometric methods (total phenolic and total flavonoid content assays). As can be seen in Table 3, a total of twenty-one phenolic compounds were quantified in at least one sample. As such, isoquercitrin was only quantified in the hydroethanolic extract of sloe skins, while gallic acid, coumaric acid, kaempferol 3-rutoside and hesperidin were not detected in the former. Apart from that, the flavonoids rutin, naringin, quercitrin and catechin, were found below the limit of quantification in the hydroethanolic extract of sloe seeds, as well as in both extracts in the latter polyphenol.

The main phenolic compounds quantified in sloe seeds were quercetin ((57 ± 7) $\mu g \cdot g^{-1}$), followed by several phenolic acids, namely ferulic acid, 2,3-dihydroxybenzoic acid, protocatechuate and vanillic acid, ranging between 41.5 and 23.4 $\mu g \cdot g^{-1}$. Moreover, these concentrations were significantly higher than those shown in sloe seed hydroethanolic extract, other that ferulic acid (Table 3). Largely, the composition of phenolic acids and flavonoids in the sloe skins was quite close, with 53 % of phenolic acids, compared to 49 % of flavonoids, where the contribution of quercetin, quercetin 3-arabinoside and kaempferol stands out (Table 3). Such results are in accordance with previous findings (Negrean et al., 2023), which have stated that quercetin and its glycosides, such as rutin, quercitrin, isoquercitrin, quercetin 3-arabinoside, isorhamnetin 3-rutinoside (Table 3), occur more abundant in sloe skins. Be that as it may, (Popović et al., 2020) determined quercetin at concentration range between 4.8 and 0.1 $\mu g \cdot g^{-1}$ in

Table 2
Retention time, molecular formula, MS fragmentation and name of the main compounds detected in residual *P. spinosa* skin and seed.

Peak number	RT (min)	Molecular formula	$[M-H]^-$ (*m/z*)	MS/MS fragments (m/z)	Compound
1	2.7	$C_7H_6O_5$	169.1128	169.0280; 125.0306; 97.0302; 79.0243; 51.0305	Gallic acid[a]
2	4.9	$C_7H_6O_4$	153.1138	153.0222; 125.5103; 109.0303; 91.0201; 65.006	2,3-Dihydroxybenzoic acid[a]
3	4.9	$C_{16}H_{18}O_9$	353.0879	353.0791; 191.0433; 179.0335; 161.1005; 135.0433; 107.0429	Neochlorogenic acid[b]
4	5.0	$C_7H_6O_4$	153.0194	153.0159;120.5030; 109.0351; 91.0221; 81.0410	Protocatechuate[a]
5	7.5	$C_{15}H_{14}O_6$	289.2609	289.0584; 245.0703; 203.0567; 151.0285; 109.0185; 57.0262	Catechin[a]
6	7.8	$C_{16}H_{18}O_9$	353.3015	353.0731; 319.6037; 257.5812, 191.0613; 161.0299; 85.0372	Chlorogenic acid[a]
7	9.2	$C_8H_8O_4$	167.0351	167.0502; 151.0007; 108.0227; 91.0128; 80.5217	Vanillic acid[a]
8	9.6	$C_9H_8O_4$	179.1502	179.0327; 135.0469; 117.0299, 89.0406; 65.0374	Caffeic acid[a]
9	9.7	$C_9H_{10}O_5$	197.0456	197.0406; 181.0194; 167.0176; 151.9915; 138.0294; 123.0072; 95.0121	Syringic acid[a]
10	9.8	$C_{15}H_{14}O_6$	289.2609	289.0701; 245.0839; 203.0711; 151.0428; 109.0343; 57.0379	Epicatechin[a]
11	13.8	$C_9H_8O_3$	163.1508	163.0339; 119.0516; 93.0364; 65.0359	*p*-Coumaric acid[a]
12	15.2	$C_{27}H_{30}O_{16}$	609.5103	609.1400; 458.1375; 373.0508; 301.0320; 179.0057	Rutin[a]
13	15.2	$C_{10}H_{10}O_4$	193.1768	193.0439; 0.150.0655; 134.0400; 106.0488; 89.0389	*trans*-Ferulic acid[a]
14	16.4	$C_{21}H_{20}O_{12}$	463.0883	463.0754; 377.7944; 340.7278; 300.0231; 254.9452; 181.8977	Isoquercitrin[b]
15	17.7	$C_{27}H_{30}O_{15}$	593.1513	593.1488; 423.0438; 367.7453; 285.0372; 195.1208; 61.9900	Kaempferol 3-rutinoside[b]
16	17.9	$C_{28}H_{32}O_{16}$	623.1618	623.1671; 577.2840; 315.0504; 300.0258; 271.6939; 243.0098	Isorhamnetin 3-rutinoside[c]
17	17.9	$C_{21}H_{20}O_{11}$	447.0934	447.0984; 355.7114; 314.0397; 223.8625; 161.0404; 89.0198	Quercitrin[b]
18	18.1	$C_{27}H_{32}O_{14}$	579.5274	579.1733; 459.1171; 373.0866; 271.0676; 151.0035	Naringin[a]
19	18.4	$C_{28}H_{34}O_{15}$	609.5534	609.1852; 527.2731; 459.0930; 301.0707; 257.0955; 136.0119	Hesperidin[a]
20	18.5	$C_{20}H18O_{11}$	433.0777	433.0621; 301.0329; 300.0169; 271.0108; 150.9931	Quercetin 3-arabinoside[b]
21	27.0	$C_{15}H_{10}O_7$	301.2285	301.0392; 273.0425; 229.0516; 179.0033; 151.0081; 121.0317	Quercetin[a]
22	32.6	$C_{15}H_{10}O_6$	285.2291	285.0394; 255.0218; 229.0400; 185.0529; 151.0335; 93.0308	Kaempferol[a]

Data contrasted with commercial standard[a], FooDB[b] and MassBank[c] database.

Table 3
Phenolic content of hydroalcoholic extracts of residual sloe skins and seeds determined by HPLC-ESI-QTOF and spectrophotometric methods.

	Sloe skins	Sloe seeds
Total indexes		
TPC (mg GAE·g^{-1})	0.7 ± 0.1*	0.25 ± 0.02
TFC (mg QE·g^{-1})	3.7 ± 0.6*	1.51 ± 0.06
Individual compounds (μg·g^{-1} sample)		
Gallic acid [A]	*n.d.*	1.4 ± 0.2
2,3-Dihydroxybenzoic acid [B]	30 ± 3*	9.70 ± 0.06
Neochlorogenic acid [C]	9.2 ± 0.7	12.9 ± 0.9*
Protocatechuate [B]	28 ± 5*	9.67 ± 0.06
Catechin	*n.q.*	*n.q.*
Chlorogenic acid [C]	0.92 ± 0.01	5.3 ± 0.5**
Vanillic acid [B]	23 ± 3**	1.11 ± 0.03
Caffeic acid [C]	0.52 ± 0.08	4.5 ± 0.2**
Syringic acid [A]	2.4 ± 0.3*	0.54 ± 0.06
Epicatechin [E]	*n.q.*	0.5 ± 0.1
p-Coumaric acid [F]	*n.d.*	19.7 ± 0.3
Rutin [G]	5 ± 1	*n.q.*
trans-Ferulic acid [H]	42 ± 4	35 ± 2
Isoquercitrin [I]	3.9 ± 0.7	*n.d.*
Kaempferol 3-rutinoside [J]	*n.d.*	1.25 ± 0.02
Isorhamnetin 3-rutinoside [I]	4.1 ± 0.1**	1.5 ± 0.1
Quercitrin [I]	5.5 ± 0.5	*n.q.*
Naringin [K]	4.2 ± 0.8	*n.q.*
Hesperidin [L]	*n.d.*	1.31 ± 0.08
Quercetin 3-arabinoside [I]	25.5 ± 0.6**	1.365 ± 0.003
Quercetin [I]	57 ± 7**	15 ± 2
Kaempferol [J]	14 ± 4*	1.3 ± 0.1
Total phenolic acids (μg·g^{-1} sample)	140 ± 10*	99.7 ± 0.9
Total flavonoids (μg·g^{-1} sample)	120 ± 20*	22 ± 2
Total phenolics (μg·g^{-1} sample)	250 ± 50*	122 ± 7

Data expressed as the mean ± standard deviation (SD) of three independent experiments. * *p*-value <0.05; **p-value <0.01 according to two-paired *t*-Student test.
A – gallic acid (LOD = 8.6 μg·L^{-1}, LOQ = 28.7 μg·L^{-1}); B – 2,3-dyhydroxibenzoic acid (LOD = 1.1 μg·L^{-1}, LOQ = 3.7 μg·L^{-1}); C – caffeic acid (LOD = 2.5 μg·L^{-1}, LOQ = 8.3 μg·L^{-1}); D – catechin (LOD = 0.9 μg·L^{-1}, LOQ = 3.0 μg·L^{-1}); E – epicatechin (LOD = 0.8 μg·L^{-1}, LOQ = 2.7 μg·L^{-1}): F – *p*-coumaric acid (LOD = 1.1 μg·L^{-1}, LOQ = 3.7 μg·L^{-1}); G – rutin (LOD = 2.0 μg·L^{-1}, LOQ = 6.7 μg·L^{-1}); H – *trans*-ferulic acid (LOD = 1.7 μg·L^{-1}, LOQ = 5.7 μg·L^{-1}); I – quercetin (LOD = 1.4 μg·L^{-1} and LOQ = 4.7 μg·L^{-1}); J – kaempferol (LOD = 1.4 μg·$L^{-1}$and LOQ = 4.7 μg·L^{-1}); K – naringin (LOD = 0.8 μg·L^{-1}, LOQ = 2.7 μg·L^{-1}); L – hesperidin (LOD = 0.3 μg·L^{-1}, LOQ = 0.1 μg·L^{-1}); *n.d.* = not detected; *n.q.* = not quantified.

blackthorn fruits after performing a maceration at 40 °C and sonication with 50:50 (*v*/v) ethanol-water, which could be attributed to the minor abundance of the flavonoid in these samples, coupled with the lower extraction efficiency compared to the MSPD method employed in this study.

As for the sloe seed extracts, ferulic acid was the main one, with a concentration of (35 ± 2) μg·g^{-1}, while coumaric acid, quercetin, neochlorogenic acid, 2,3-dihydroxybenzoic acid and protocatechuate were determined between 19.7 and 9.67 μg·g^{-1}, albeit all of them at concentrations significantly equal or lower than those found in the sloe skins, apart from coumaric and neochlorogenic acids (Table 3). In addition, chlorogenic acid and caffeic acid were recorded at around 5 μg·g^{-1}, placing them at an intermediate abundance among the compounds quantified in sloe seed. Resembling the distribution of phenolic families observed in the sloe skins, phenolic acids predominated over flavonoids (Table 3), with much more disparate percentages, 82 % and 18 % of the total content, respectively. In this regard, (Damar & Yilmaz, 2023; Najgebauer-Lejko et al., 2021) remarked chlorogenic, caffeic, coumaric and ferulic acids *versus* flavonoids in sloe fruits and puree. In addition, (Damar & Yilmaz, 2023) determined ferulic, protocatechuic, caffeic and coumaric acid in hydrolyzed extracts of sloe fruits, in the same order of magnitude (0.7–38.6 μg·g^{-1}) as this study.

Overall, sloe skins appear to be a richer source of phenolic compounds, with a total concentration twice that found in seeds (250 μg·g^{-1} *vs.* 122 μg·g^{-1}). Yet, both sloe residues remain fruitful reservoirs of quercetin, ferulic acid and 2,3-dihydroxybenzoic acid, which have been correlated with several biological effects on human health, including neuroprotective aspects (Gómez-Mejía, Vicente-Zurdo, et al., 2022).

3.3.2. Total phenolic contents

As for spectrophotometric determinations, namely TPC and TFC, both are widely applied in the analysis of phenolic compounds in agri-food matrices, as providing rapid and useful information on the variability of phenolic composition (León-González et al., 2018). Table 3 includes the TPC and TFC values obtained for sloe residue extracts. As can be seen, both, TPC and TFC were significantly higher in sloe skin hydroethanolic extract, in agreement with chromatographic data. On the other hand, (Opriş et al., 2021) revealed a TPC of 1.02 mg GAE·g^{-1} in hydroethanolic extracts of sloe fruits obtained by UAE with heating, a value higher than that established herein for isolated sloe residues (0.25 mg GAE·g^{-1} and 0.7 mg GAE·g^{-1} for sloe seed and skins, respectively),

yet together almost comparable. Furthermore, (Velickovic et al., 2016) determined a TFC of (0.42 ± 0.013) mg QE·g^{-1} in aqueous extract of *P. spinosa* fruits, significantly lower than that of seed ((1.51 ± 0.06) mg QE·g^{-1}) and skin ((3.7 ± 0.6) mg QE·g^{-1}) MSPD hydroethanolic extracts.

Eventually, it is noteworthy to mention that the samples of this study are a bio-residue, whose phenolic composition has most likely migrated during the preparation of the liquor (Popović et al., 2020), so that concentration values similar to those reported in other studies, denotes not only the potential of the extraction method, but also of the bio-residue itself to be valorized as a source of phenolic compounds.

3.4. *In vitro antioxidant activity of sloe phenolic extracts in SH-SY5Y cell line*

Assessing antioxidant performance is a crucial aspect of research into potential treatments for neurodegenerative diseases, as oxidative stress, resulting from an imbalance between reactive oxygen and nitrogen species and the body's antioxidant defenses, can cause oxidative damage to cellular structures and cell death (Silva & Pogačnik, 2020). Moreover, the central nervous system, being the most metabolically active organ, produces a large amount of superoxide radical anion, hydroxyl radical and hydrogen peroxide, which makes it particularly vulnerable to oxidative stress and reactive oxygen species damage (Moyano et al., 2021). The human neuroblastoma cell line (SH-SY5Y) is commonly used in neuroscience investigation due to its neuronal-like characteristics (Saini et al., 2022). Thus, when subjected to oxidative stress, these cells can show reduced viability and altered morphology (Bhattamisra et al., 2020), making them a relevant and ideal model to evaluate the antioxidant effects of any compound, including phenolic compounds from sloe residues.

3.4.1. *Effect of sloe extracts on cell viability and optimization of trolox and H_2O_2 concentrations*

Prior to any cytoprotective study against oxidative stress, the inherent cytotoxicity of the potential agents should be evaluated (Moyano et al., 2021). For this purpose, SH-SY5Y cells were incubated, for 48 h, in the presence of phenolic extracts of sloe skin and seed at different concentrations (0.001 μg·L^{-1}, 1 μg·L^{-1}, 1 mg·L^{-1}, 80 mg·L^{-1}, 400 mg·L^{-1} and 2000 mg·L^{-1}). Cell viability was significantly reduced above 80 mg·L^{-1} (data not shown), so that a safe interval could be established, *i.e.*, a cell viability statistically similar to that of the control with a confidence level of 95 %, for the application of both phenolic extracts ranging from 0.001 to 1000 μg·L^{-1}.

In this study, oxidative stress was induced in cells by the addition of a reactive oxygen species, to be hydrogen peroxide. Thus, to establish the protective effect of phenolic extracts against oxidative stress injury, it was necessary to determine the concentration of H_2O_2 that led to a significant, yet not total, reduction in cell population. For this purpose, SH-SY5Y cells were exposed to increasing H_2O_2 concentrations for a period of 48 h, revealing their vulnerability to oxidative stress caused by H_2O_2. The cytotoxicity of SH-SY5Y cells to H_2O_2 was seen to be dose-dependent, within a concentration spectrum of 200–1000 μM over 48 h of incubation, with almost no survival at the highest concentration (Fig. 1a). As a result, H_2O_2 concentration of 600 μM, leading to a cell viability value of (35 ± 7) %, was selected to examine the protective antioxidant properties of sloe skin and seed extracts.

Afterwards, co-incubation of 600 μM of H_2O_2 with trolox at various concentrations (25–900 μM), was measured, as an antioxidant standard compound, to find trolox optimal concentration with the highest cell viability. According to one-way ANOVA test, significant differences between the concentrations studied were observed. Additionally, the Duncan's test was applied to reveal between which groups exist differences with respect to the control.

As can be noticed in Fig. 1b, trolox at no concentration was able to fully reverse the oxidative stress induced by H_2O_2, not reaching cell viability levels statistically comparable to the control, according to ANOVA and Duncan multiple comparison test. Whereas, at the lowest trolox concentrations, cell viability did not differ statistically from H_2O_2-treated cells, a significant increase was observed at 400 μM, continuing up to 550 μM, with a cell viability of (60 ± 6) %. However, above this concentration no significant differences were noted (Fig. 1b), therefore 550 μM concentration of trolox was chosen for comparison purposes.

3.4.2. *Cytoprotective effect of sloe extracts against oxidative stress*

Regarding the effect of the sloe extracts on the cytotoxicity induced by oxidative stress, both extracts conferred a degree of protection against cell death induced by H_2O_2, exhibiting a dose-responsive relationship (Fig. 2). However, none of them completely counteracted the cytotoxicity of hydrogen peroxide, failing to reach levels comparable to the untreated control (p-value <0.05), within the range evaluated. As it can be seen in Fig. 2, the phenolic extract of sloe skin was able to increase cell viability above 50 %, at concentrations of 1 μg·L^{-1} ((59 ± 9) %) and 10 μg·L^{-1} ((73 ± 9) %), counteracting the oxidative stress caused by H_2O_2 ((35 ± 5) %). This cytoprotection was statistically similar to that obtained in the treatment of 550 μM of trolox ((60 ± 2) %), while

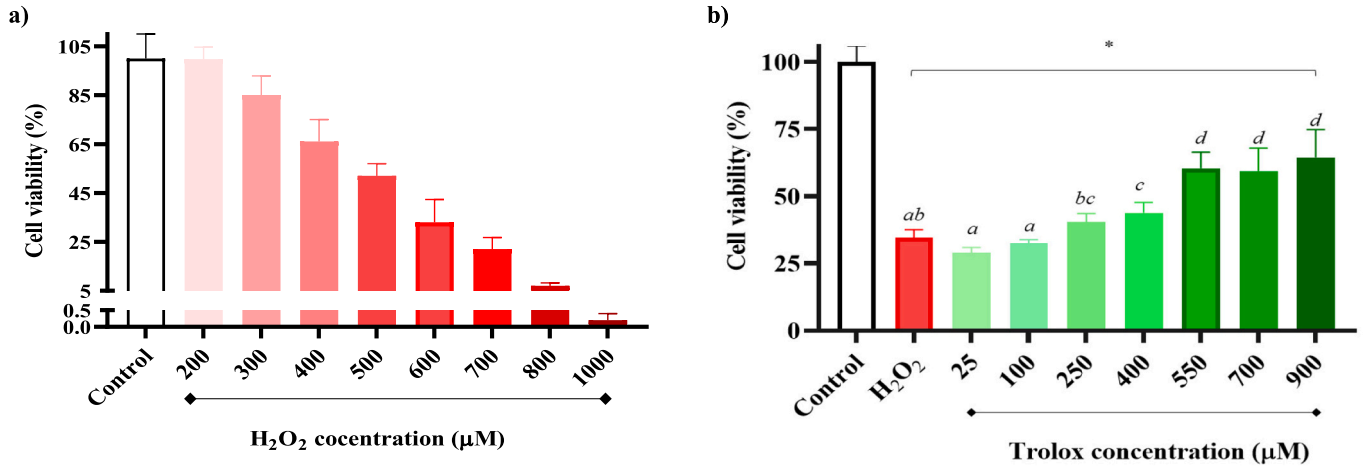

Fig. 1. Effects on cell viability of the neuroblastoma line SH-SY5Y after treatment with (a) H_2O_2 (10–100 μM), (b) H_2O_2 (600 μM) and trolox (25–900 μM), measured by MTT method. Data represent the mean ± SD of three independent experiments in quintuplicate. *p-value ≤0.05 compared to control. Mean values with different letters indicate significant differences between groups (p-value ≤0.05).

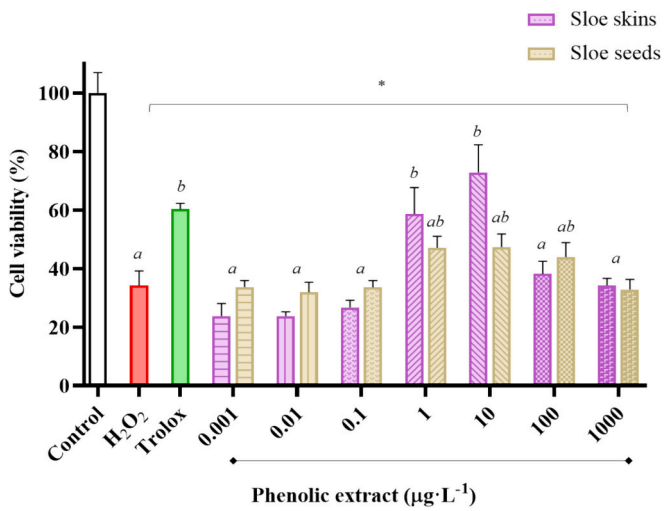

Fig. 2. Cell viability measured by MTT assay in H_2O_2-induced oxidative stress on SH-SY5Y line with phenolic extracts of sloe seeds and skins (0.001 to 1000 $\mu g \cdot L^{-1}$). H_2O_2 (600 μM); trolox (550 μM). Data represent the mean ± SD of three independent experiments in quintuplicate. *p-value ≤0.05 compared to control. Mean values with different letters indicate significant differences between groups (p-value ≤0.05).

presenting significant differences with respect to cells incubated only with H_2O_2. As such, these results demonstrate the antioxidant effectiveness of sloe skin extracts in protecting neuronal cells against oxidative stress. When it comes to the phenolic extract of sloe skin, within the concentration range of 1 to 100 $\mu g \cdot L^{-1}$, a boost in cell viability was noticed, ranging from 44 % to 47 %. Nevertheless, remaining statistically similar to the viability obtained in cells treated solely with H_2O_2 (Fig. 2), thus, no antioxidant potential of the sloe seed extract could be demonstrated within the range of concentrations tested.

The antioxidant effects of phenolic extracts derived from plant-derived matrices on the SH-SY5Y against H_2O_2-induced oxidative stress have been investigated by other authors. (Palmioli et al., 2022) examined the impact of four extracts from different varieties of hops (*Humulus lupulus* L.), obtained through conventional solid-liquid extraction (SLE) with 10 % ethanol. Pretreatment of SH-SY5Y cells for 1 h with hop extract concentrations of 0.1 and 0.25 $mg \cdot mL^{-1}$ partially mitigated the cytotoxicity induced by 100 μM H_2O_2, achieving a cell viability up to 95 %. Additionally, (Sayuti et al., 2023) investigated the neuroprotective effect of the medicinal plant phenolic extract *Polygonum minus*, obtained by SLE with ethanol. In their study, SH-SY5Y cells were treated with varying concentrations of phenolic extracts, ranging from 0.5 to 1000 $\mu g \cdot mL^{-1}$, prior to the induction of oxidative stress with 220 μM H_2O_2. The results revealed that pretreatment with *P. minus* phenolic extract provided significant protection against the cytotoxic effects of H_2O_2, particularly at a concentration of 62.5 $\mu g \cdot mL^{-1}$, enhancing cell viability from approximately 50 % to 75 %. While the results of these studies are notable, the concentrations used are significantly higher than those presented herein (0.001 $\mu g \cdot L^{-1}$ and 1 $mg \cdot L^{-1}$), underscoring the superior efficacy of sloe extracts as antioxidant agents.

In general, the inhibitory effects of sloe phenolic extracts could be corroborated by the phenolic composition previously documented in the hydroalcoholic extracts of both residues (Table 3). Consequently, sloe skin extract exhibited a higher concentration of phenolic compounds, particularly quercetin, 2,3-dihydroxybenzoic acid, protocatechuate, kaempferol, and vanillic acid, in addition to ferulic acid, which was abundantly present in both residues. Accordingly, (Zhang et al., 2008) identified that the standard quercetin exerted the greatest protection (EC_{50} = 0.29 μM) against H_2O_2-induced cell death in the SH-SY5Y line. Likewise, the *in vitro* antioxidant role of rutin, ferulic and kaempferol was noted, although with lower efficacy (EC_{50} = 0.87–2.7 μM), which could account for the improved antioxidant effectiveness of sloe skins, compared to seeds (Zhang et al., 2008). Moreover, the antioxidant potential of phenolic compounds in SH-SY5Y models is attributed not only to their ability to neutralize or scavenge reactive oxygen species but also to their activation of antioxidant signaling pathways, such as Nrf2/ARE, NF-κB/IκB, and MAPK, thereby reducing neuronal damage and death (Sayuti et al., 2023). Further to this, the presence of Cu in the sloe seed extract (Table 1) could potentially contribute to its inferior performance against oxidative stress, given its role in promoting oxidation *via* the Fenton reaction and inducing neuronal cell death (Chen et al., 2023; Moyano et al., 2021). In this context, (Moyano et al., 2021) documented a paramount decline, approximately 50 %, in the viability of neuronal SN56 cells after their exposure to 20 μM $CuCl_2$.

3.5. Anti-amyloidogenic properties of sloe extracts against Alzheimer's disease

Complementarily to the *in vitro* antioxidant activity, the potentiality of phenolic extracts derived from the peel and seeds of sloe as agents against AD has been also evaluated, with a specific focus on their influence on the aggregation of $A\beta_{42}$. In this assay, 50 μM curcumin was used as a negative control against $A\beta_{42}$ aggregation, due to its recognized anti-amyloidogenic properties (Tang & Taghibiglou, 2017). Fig. 3 illustrates the TEM micrographics collected after $A\beta_{42}$ incubation in each condition studied.

To test the absence of amyloidogenic activity of sloe extracts, $A\beta_{42}$ was incubated with 1 $\mu g \cdot L^{-1}$ skin and seed sloe extracts in absence of Fe (II). The 1 $\mu g \cdot L^{-1}$ concentration was selected based on the significant increase in cell viability against oxidative stress, of cells treated with sloe skin phenolic extract. As a result, neither skin extract (Fig. 3b) nor seed extract (Fig. 3c) demonstrated a rise in amyloid aggregation when compared to $A\beta_{42}$ alone (Fig. 3a), indicating that none of the two extracts exacerbated aggregation under normal conditions. On the other hand, fibrils width suffered a slightly widening when incubated with skin ((7.8 ± 0.8) nm) and seed ((6.7 ± 0.8) nm) extracts, in comparison with $A\beta_{42}$ alone ((4.5 ± 0.6) nm), finding significant differences between all of them according to one-way ANOVA and Duncan's multiple comparison.

Conversely, after 48 h of $A\beta_{42}$ incubation with Fe(II), amyloid plaque formation occurred (Fig. 3d) and fibrils acquired their maximum width value ((9 ± 1) nm). This behavior was entirely prevented when incubating with both sloe skin (Fig. 3e) and seed (Fig. 3f) extracts, which effectively curtailed $A\beta_{42}$ aggregation and reduced fibrils width (p-value <0.05) to (7 ± 1) nm and (8 ± 1) nm, respectively, thereby thwarting the "metal ion hypothesis" associated with AD progression.

Overall, sloe skin extract showed a better capacity to inhibit Fe(II)-induced amyloid aggregation, therefore reducing $A\beta_{42}$ aggregation to a greater extent than the seed extract. This fact could be explained by several reasons. Firstly, sloe seed extract presented a higher content of metals such as Cu and Zn, while they were not present in the skin extract. Given that these metals are related to increased amyloid aggregation (Chen et al., 2023), this may be a limiting factor for the inhibition by this type of extract. Secondly, as stated in the *in vitro* assays with SH-SY5Y cell line, skin extract proved to be more antioxidant than seed extract (Fig. 2). Since oxidative stress induced by metal ions is one of the key factors that promotes amyloid aggregation, the higher antioxidant capacity of skin extract could favor amyloid inhibition. Thus, the predominant presence of 2,3-dihydroxybenzoic acid, trans-ferulic acid and quercetin, all being demonstrated *in vitro* antioxidant compounds (Gómez-Mejía, Rosales-Conrado, et al., 2022; Zhang et al., 2008), could contribute to the inhibitory effect of these extracts, to a greater extent in sloe skins. On the other hand, several studies have demonstrated the chelating role of quercetin (stoichiometry 1:1) and *trans*-ferulic acid (stoichiometries 1:1 and 1:2) against iron (Filipský et al., 2013; Truong et al., 2020), which could contribute to the higher efficacy of $A\beta_{42}$ protein aggregation inhibition in the skin extract.

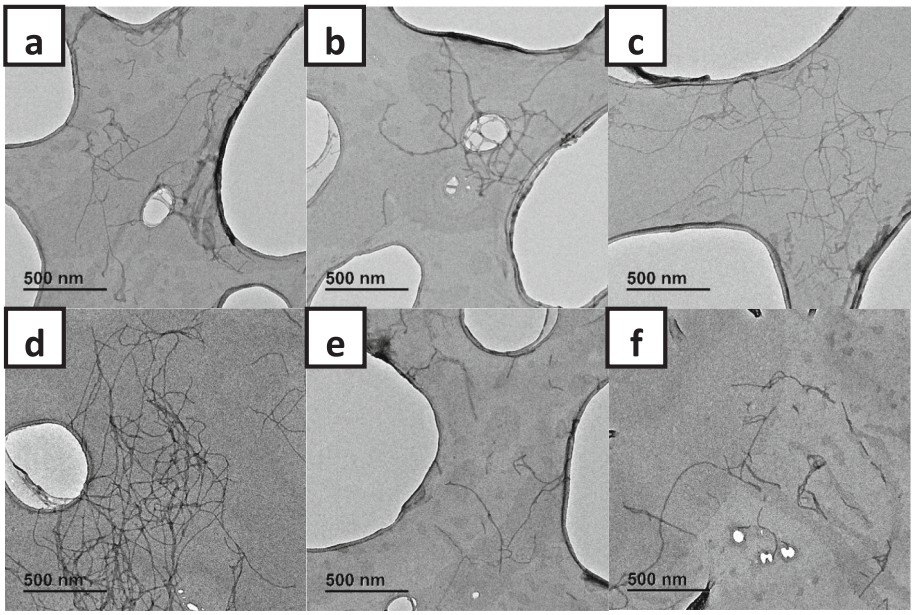

Fig. 3. TEM micrographs of 50 μM $A\beta_{42}$ incubated at 37 °C for 48 h in 10 mM HCl: a) $A\beta_{42}$ alone; b) $A\beta_{42}$ plus 1 $\mu g \cdot L^{-1}$ skin extract; c) $A\beta_{42}$ plus 1 $\mu g \cdot L^{-1}$ seed extract; d) $A\beta_{42}$ plus 50 μM Fe(II); e) $A\beta_{42}$ plus Fe(II) plus skin extract; f) $A\beta_{42}$ plus Fe(II) plus seed extract, at the aforementioned concentrations.

In a previous study, grape seed phenolic extract, rich in catechin, 2,3-dihydroxybenzoic acid, gallic acid and quercetin, obtained through the same MSPD procedure described herein, demonstrated the capacity to inhibit Fe(II)-induced amyloid aggregation (Gómez-Mejía, Vicente-Zurdo, et al., 2022). Although the $A\beta_{42}$ and Fe(II) experimental conditions were identical to those employed in this study, the concentrations of grape seed phenolic extract (14.5–58 $\mu g \cdot L^{-1}$) were four orders of magnitude higher than those tested on sloe extracts (1 $\mu g \cdot L^{-1}$). Conversely, (Palmioli et al., 2022) demonstrated that phenolic extracts derived from hops at a concentration of 0.25 $mg \cdot mL^{-1}$ were capable of inhibiting $A\beta_{42}$ aggregation at 2.5 μM by up to 99 %. However, this study did not address the influence of amyloidogenic promoters such as Fe, and the extract concentration used was fivefold higher than that of sloe (1 $\mu g \cdot L^{-1}$). This comparison underscores the potent anti-amyloidogenic activity of sloe phenolic extracts relative to other extracts documented in the literature, highlighting their protective role against amyloidogenic agents such as Fe(II) ions.

3.6. Multivariate study by principal component analysis

To correlate the antioxidant activity, anti-amyloidogenic activity and phenolic indices (TPC and TFC) with the phenolic and metal profile in the hydroalcoholic extracts of the samples, a multivariate analysis by PCA was carried out. Fe and catechins were not included in the PCA analysis given that they could not be quantified in either sample. Conversely, the anti-amyloidogenic activity was expressed as the fiber width in the iron-incubated samples for each of the extracts; and the antioxidant activity was expressed as the cytoprotection offered (cell viability) by 1 $\mu g \cdot L^{-1}$ of the sloe extracts against oxidative stress. The PCA has facilitated the reduction of the 28 variables examined to two primary components, which explain 98.4 % of the total variance. The resulting bi-graph is presented in Fig. 4, where samples are clustered into two main groups, revealing a composition pattern and significant differences between the sloe residues, mainly explained by the first component (Fig. 4), whereas the second one primarily explains the variability inherent within the samples, being higher in skins (Fig. 4).

In accordance with the loading directions, various relationships can be established. The sloe seed extract was categorized by

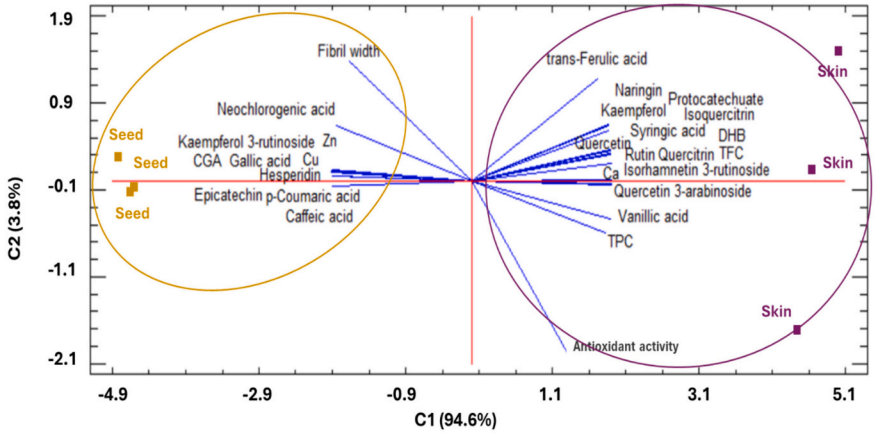

Fig. 4. Principal Component Analysis bi-plot of the simultaneous evaluation of the loadings (individual phenolic concentration, TPC, TFC, antioxidant activity and fibril width) and scores (sloe residues) studied. CGA: chlorogenic acid. DHB: 2,3-dihydroxybenzoic acid.

hydroxycinnamic acids, except for ferulic acid, as well as hesperidin, kaempferol, epicatechin, and the metals Zn and Cu; along with a greater width of $A\beta_{42}$ protein (Fig. 4). Alternatively, the sloe skin extract was richer in flavonoids, highlighting quercetin and its derivatives (rutin, isoquercitrin, quercetin 3-arabinoside…), and in hydroxybenzoic acids (2,3-dihydroxybenzoic acid, protocatechuate, syringic and vanillic acid). Moreover, it exhibited higher values of TPC, TFC, and Ca, as well as higher antioxidant potential (Fig. 4). Furthermore, most parameters are situated in close proximity to each other, which signifies high positive correlations among them. Particularly, a remarkable correlation between TPC and vanillic acid was observed, as well as between TFC and quercetin, rutin, and quercitrin stands out, in accordance with previous studies on grape residues (Gómez-Mejía et al., 2021). Moreover, an inverse relationship between the width of the fibers and the antioxidant activity can be noticed in Fig. 4**.** Where, according to the first component, the cytoprotective effect against oxidative stress could be attributed to quercetin-like flavonoids and to the hydroxybenzoic acids previously mentioned. Similarly, (Popović et al., 2020; Zhang et al., 2008) described that those flavonoids containing the catechol structure, as in the case of quercetin, were more antioxidant by different methods, being known to be responsible for free radical scavenging properties.

4. Conclusions

This study has focused on the valorization of sloe (*P. spinosa*) residues, produced post the manufacturing of liqueur, utilizing an economical, efficient and straightforward MSPD green extraction, for the development of neuroprotective agents, remarking the inaugural characterization of both phenomena.

Both hydroethanolic extracts, derived from sloe skins and seeds, were notably rich in quercetin and its derivatives (16–96 $\mu g \cdot g^{-1}$), along with 2,3-dihydroxybenzoic acid (10–30 $\mu g \cdot g^{-1}$) and ferulic acid (35–42 $\mu g \cdot g^{-1}$). A significant richness was observed in sloe skins, which also exhibited the highest total phenolic and flavonoid contents. Moreover, sloe phenolic extracts contained Cu (4.7 $\mu g \cdot g^{-1}$), while the essential mineral Ca was identified in the phenolic extract of sloe skin (0.102 $mg \cdot g^{-1}$), thereby enhancing the added value of peel extract as a functional ingredient.

Furthermore, the anti-amyloidogenic properties exhibited by both, sloe skin and seed extracts at 1 $\mu g \cdot L^{-1}$, and the potent antioxidant activity displayed by sloe skin extract at 1 and 10 $\mu g \cdot L^{-1}$ concentration levels, against H_2O_2-induced oxidative stress on human neuroblastoma SH-SY5Y cell, which were subsequent correlated with the phenolic composition of the former, may provide fresh insights into their applicability as neuroprotective agents.

The analytical strategy implemented is aligned with the principles of green chemistry for the recovery and characterization of bioactive compounds obtained from agri-food bio-residues, as well as the circular economy concept and the Sustainable Development Goals, offering potential industrial applications.

Overall, this research supports that sloe residues, namely sloe skins, are an unexplored yet intriguing source of phenolic compounds with promising potential in the treatment and management of different neurodegenerative diseases. Despite these promising results, further research is imperative to assess the eco-friendliness and scalability of the extraction methodology. Additionally, it is essential to investigate the permeability of the compounds across the blood-brain barrier and to explore other neuroprotective mechanisms, such as the inhibition of acetylcholinesterase enzymes, through *in vivo* studies. These efforts would be crucial to substantiate and provide more reliable information on the neuroprotective potential of sloe phenolic extracts.

CRediT authorship contribution statement

Esther Gómez-Mejía: Writing – review & editing, Writing – original draft, Visualization, Validation, Methodology, Investigation, Formal analysis, Data curation, Conceptualization. **David Vicente-Zurdo:** Writing – review & editing, Writing – original draft, Visualization, Validation, Methodology, Investigation, Formal analysis, Data curation, Conceptualization. **Noelia Rosales-Conrado:** Writing – review & editing, Visualization, Supervision, Resources, Project administration, Funding acquisition, Conceptualization. **María Eugenia León-González:** Writing – review & editing, Visualization, Supervision, Conceptualization.

Declaration of competing interest

The authors declare that they have no known competing financial interests or personal relationships that could have appeared to influence the work reported in this paper.

Data availability

Data will be made available on request.

Acknowledgements

The authors acknowledge Hijos de Pablo Esparza Bodegas Navarras S.A. company for providing the sloe samples. This work was supported by the Complutense University of Madrid [PR26/16-16B-3], the Community of Madrid/FEDER program [S2018/BAA-4393, AVANSECAL II-CM] and the Ministry of Science, Innovation and Universities [project PID 2020-114714RB- I00 and PID2023-149424OB-I00].

References

AOAC International. (2000). *Official methods of analysis of AOAC INTERNATIONAL.* Gaithersburg, MD, USA: Official Method 925.10.

AOAC International. (2003). *Official methods of analysis of AOAC INTERNATIONAL.* Gaithersburg, MD, USA: Official Method 923.03.

Babalau-Fuss, V., Bogdana Grebla, O., Cadar, O., Hoaghia, M.-A., Kovacs, M.-H., Moldovan, A., & Tofana, M. (2018). *Determination of chemical composition and fatty acids of blackthorn fruits (Prunus spinosa) grown near Cluj-napoca, NW Romania.*

Barros, A., Gouvinhas, I., Machado, N., Pinto, J., Cunha, M., Rosa, E., & Domínguez-Perles, R. (2016). New grape stems-based liqueur: Physicochemical and phytochemical evaluation. *Food Chemistry, 190*, 896–903. https://doi.org/10.1016/j.foodchem.2015.06.047

Bhattamisra, S. K., Shak, A. T., Xi, L. W., Safian, N. H., Choudhury, H., Lim, W. M., … Md, S. (2020). Nose to brain delivery of rotigotine loaded chitosan nanoparticles in human SH-SY5Y neuroblastoma cells and animal model of Parkinson's disease. *International Journal of Pharmaceutics, 579*. https://doi.org/10.1016/j.ijpharm.2020.119148

Capaldi, G., Binello, A., Aimone, C., Mantegna, S., Grillo, G., & Cravotto, G. (2024). New trends in extraction-process intensification: Hybrid and sequential green technologies. *Industrial Crops and Products, 209*, Article 117906. https://doi.org/10.1016/j.indcrop.2023.117906

Castillo, A., Celeiro, M., Rubio, L., Bañobre, A., Otero-Otero, M., Garcia-Jares, C., & Lores, M. (2022). Optimization of bioactives extraction from grape marc via a medium scale ambient temperature system and stability study. *Frontiers in Nutrition, 9*, 1008457. https://doi.org/10.3389/FNUT.2022.1008457

Chen, L. L., Fan, Y. G., Zhao, L. X., Zhang, Q., & Wang, Z. Y. (2023). The metal ion hypothesis of Alzheimer's disease and the anti-neuroinflammatory effect of metal chelators. *Bioorganic Chemistry, 131*, Article 106301. https://doi.org/10.1016/j.bioorg.2022.106301

Damar, I., & Yilmaz, E. (2023). Ultrasound-assisted extraction of phenolic compounds in blackthorn (*Prunus spinosa* L.): Characterization, antioxidant activity and optimization by response surface methodology. *Journal of Food Measurement and Characterization, 17*(2), 1467–1479. https://doi.org/10.1007/s11694-022-01723-5

Du, L. J., Huang, J. P., Wang, B., Wang, C. H., Wang, Q. Y., Hu, Y. H., … Zhang, Q. D. (2018). Carbon molecular sieve based micro-matrix-solid-phase dispersion for the extraction of polyphenols in pomegranate peel by UHPLC-Q-TOF/MS. *Electrophoresis, 39*(17), 2218–2227. https://doi.org/10.1002/ELPS.201800045

Farag, M. A., Bahaa Eldin, A., & Khalifa, I. (2022). Valorization and extraction optimization of *Prunus* seeds for food and functional food applications: A review with further perspectives. *Food Chemistry, 388*, Article 132955. https://doi.org/10.1016/j.foodchem.2022.132955

Filipský, T., Říha, M., Hrdina, R., Vávrová, K., & Mladěnka, P. (2013). Mathematical calculations of iron complex stoichiometry by direct UV–vis spectrophotometry. *Bioorganic Chemistry, 49*, 1–8. https://doi.org/10.1016/j.bioorg.2013.06.002

Gómez-Mejía, E., Mikkelsen, L. H., Rosales-Conrado, N., León-González, M. E., & Madrid, Y. (2021). A combined approach based on matrix solid-phase dispersion extraction assisted by titanium dioxide nanoparticles and liquid chromatography to

determine polyphenols from grape residues. *Journal of Chromatography A, 1644*. https://doi.org/10.1016/j.chroma.2021.462128

Gómez-Mejía, E., Rosales-Conrado, N., León-González, M. E., & Madrid, Y. (2019). Determination of phenolic compounds in residual brewing yeast using matrix solid-phase dispersion extraction assisted by titanium dioxide nanoparticles. *Journal of Chromatography A, 1601*, 255–265. https://doi.org/10.1016/j.chroma.2019.05.009

Gómez-Mejía, E., Rosales-Conrado, N., León-González, M. E., Valverde, A., & Madrid, Y. (2022). A combined analytical-chemometric approach for the *in vitro* determination of polyphenol bioaccessibility by simulated gastrointestinal digestion. *Analytical and Bioanalytical Chemistry, 414*(8), 2739–2755. https://doi.org/10.1007/s00216-022-03922-x

Gómez-Mejía, E., Sacristán, I., Rosales-Conrado, N., León-González, M. E., & Madrid, Y. (2023). Valorization of *Citrus reticulata* Blanco peels to produce enriched wheat bread: Phenolic bioaccessibility and antioxidant potential. *Antioxidants, 12*(9), 1742. https://doi.org/10.3390/antiox12091742

Gómez-Mejía, E., Vicente-Zurdo, D., Rosales-Conrado, N., León-González, M. E., & Madrid, Y. (2022). Screening the extraction process of phenolic compounds from pressed grape seed residue: Towards an integrated and sustainable management of viticultural waste. *LWT, 169*, Article 113988. https://doi.org/10.1016/J.LWT.2022.113988

Karran, E., & De Strooper, B. (2016). The amyloid cascade hypothesis: Are we poised for success or failure? *Journal of Neurochemistry, 139*, 237–252. https://doi.org/10.1111/JNC.13632

Kumarasamy, Y., Cox, P. J., Jaspars, M., Nahar, L., & Sarker, S. D. (2003). Cyanogenic glycosids from *Prunus spinosa* (Rosaceae). *Biochemical Systematics and Ecology, 31*(9), 1063–1065. https://doi.org/10.1016/S0305-1978(03)00063-2

León-González, M. E., Gómez-Mejía, E., Rosales-Conrado, N., & Madrid-Albarrán, Y. (2018). Residual brewing yeast as a source of polyphenols: Extraction, identification and quantification by chromatographic and chemometric tools. *Food Chemistry, 267*, 246–254. https://doi.org/10.1016/j.foodchem.2017.06.141

Magiera, A., Czerwińska, M. E., Owczarek, A., Marchelak, A., Granica, S., & Olszewska, M. A. (2022). Polyphenol-enriched extracts of *Prunus spinosa* fruits: Anti-inflammatory and antioxidant effects in human immune cells ex vivo in relation to phytochemical profile. *Molecules, 27*(5). https://doi.org/10.3390/molecules27051691

Mezeiova, E., Chalupova, K., Nepovimova, E., Gorecki, L., Prchal, L., Malinak, D., … Korabecny, J. (2019). Donepezil derivatives targeting amyloid-β; Cascade in Alzheimer's disease. *Current Alzheimer Research, 16*(9), 772–800. https://doi.org/10.2174/1567205016666190228122956

Moyano, P., Vicente-Zurdo, D., Blázquez-Barbadillo, C., Menéndez, J. C., González, J. F., Rosales-Conrado, N., & Del Pino, J. (2021). Neuroprotective action of multitarget 7-Aminophenanthridin-6(5H)-one derivatives against metal-induced cell death and oxidative stress in SN56 cells. *ACS Chemical Neuroscience, 12*(18), 3358–3372. https://doi.org/10.1021/acschemneuro.1c00333

Najgebauer-Lejko, D., Liszka, K., Tabaszewska, M., & Domagała, J. (2021). Probiotic yoghurts with sea buckthorn, elderberry, and sloe fruit purees. *Molecules, 26*(8), 2345. https://doi.org/10.3390/molecules26082345

Negrean, O. R., Farcas, A. C., Pop, O. L., & Socaci, S. A. (2023). Blackthorn—A valuable source of phenolic antioxidants with potential health benefits. *Molecules, 28*(8), 3456. https://doi.org/10.3390/molecules28083456

Opriş, O., Soran, M. L., Lung, I., Stegarescu, A., Guţoiu, S., Podea, R., & Podea, P. (2021). Optimization of extraction conditions of polyphenols, antioxidant capacity and sun protection factor from *Prunus spinosa* fruits. Application in sunscreen formulation. *Journal of the Iranian Chemical Society, 18*(10), 2625–2636. https://doi.org/10.1007/s13738-021-02217-9

Palmioli, A., Mazzoni, V., De Luigi, A., Bruzzone, C., Sala, G., Colombo, L., … Airoldi, C. (2022). Alzheimer's disease prevention through natural compounds: Cell-free, *in vitro*, and *in vivo* dissection of hop (*Humulus lupulus* L.) multitarget activity. *ACS Chemical Neuroscience, 13*(22), 3152–3167. https://doi.org/10.1021/acschemneuro.2c00444

Pinacho, R., Cavero, R. Y., Astiasarán, I., Ansorena, D., & Calvo, M. I. (2015). Phenolic compounds of blackthorn (*Prunus spinosa* L.) and influence of *in vitro* digestion on their antioxidant capacity. *Journal of Functional Foods, 19*, 49–62. https://doi.org/10.1016/J.JFF.2015.09.015

Popović, B. M., Blagojević, B., Ždero Pavlović, R., Mićić, N., Bijelić, S., Bogdanović, B., … Serra, A. T. (2020). Comparison between polyphenol profile and bioactive response in blackthorn (*Prunus spinosa* L.) genotypes from North Serbia-from raw data to PCA analysis. *Food Chemistry, 302*, Article 125373. https://doi.org/10.1016/j.foodchem.2019.125373

Pozzo, L., Russo, R., Frassinetti, S., Vizzarri, F., Árvay, J., Vornoli, A., … Longo, V. (2019). Wild Italian Prunus spinosa L. fruit exerts *in vitro* antimicrobial activity and protects against *in vitro* and *in vivo* oxidative stress. *Foods, 9*(1), 5, 2020 https://doi.org/10.3390/foods9010005.

Sabatini, L., Fraternale, D., Di Giacomo, B., Mari, M., Albertini, M. C., Gordillo, B., … Colomba, M. (2020). Chemical composition, antioxidant, antimicrobial and anti-inflammatory activity of *Prunus spinosa* L. fruit ethanol extract. *Journal of Functional Foods, 67*, Article 103885. https://doi.org/10.1016/J.JFF.2020.103885

Saini, V., Singh, A., Shukla, R., Jain, K., & Yadav, A. K. (2022). Silymarin-encapsulated Xanthan gum–stabilized selenium nanocarriers for enhanced activity against amyloid fibril cytotoxicity. *AAPS PharmSciTech, 23*(5). https://doi.org/10.1208/s12249-022-02274-0

Sayuti, N. H., Zulkefli, N., Tan, J. K., Saad, N., Baharum, S. N., Hamezah, H. S., … Sarian, M. N. (2023). Ethanolic extract of *Polygonum minus* protects differentiated human neuroblastoma cells (SH-SY5Y) against H_2O_2-induced oxidative stress. *Molecules, 28*(18), 6726. https://doi.org/10.3390/molecules28186726

Silva, R. F. M., & Pogačnik, L. (2020). Polyphenols from food and natural products: Neuroprotection and safety. *Antioxidants, 9*(1), 61. https://doi.org/10.3390/antiox9010061

Sytařová, I., Orsavová, J., Snopek, L., Mlček, J., Byczyński, Ł., & Mišurcová, L. (2020). Impact of phenolic compounds and vitamins C and E on antioxidant activity of sea buckthorn (*Hippophaë rhamnoides* L.) berries and leaves of diverse ripening times. *Food Chemistry, 310*, Article 125784. https://doi.org/10.1016/j.foodchem.2019.125784

Tang, M., & Taghibiglou, C. (2017). The mechanisms of action of curcumin in Alzheimer's disease. *Journal of Alzheimer's Disease, 58*(4), 1003–1016. https://doi.org/10.3233/JAD-170188

Truong, D. H., Nhung, N. T. A., & Dao, D. Q. (2020). Iron ions chelation-based antioxidant potential vs. pro-oxidant risk of ferulic acid: A DFT study in aqueous phase. *Computational and Theoretical Chemistry, 1185*, Article 112905. https://doi.org/10.1016/j.comptc.2020.112905

Velickovic, J. M., Ilic, S., Mitic, S. S., Mitic, M. N., & Kostic, D. A. (2016). Comparative analysis of phenolic and mineral composition of hawthorn and blackthorn from Southeast Serbia. *Oxidation Communications, 39*(3–I), 2280–2290.

Vicente-Zurdo, D., Gómez-Gómez, B., Pérez-Corona, M. T., & Madrid, Y. (2019). Impact of fish growing conditions and cooking methods on selenium species in swordfish and salmon fillets. *Journal of Food Composition and Analysis, 83*, Article 103275. https://doi.org/10.1016/J.JFCA.2019.103275

Vicente-Zurdo, D., Romero-Sánchez, I., Rosales-Conrado, N., León-González, M. E., & Madrid, Y. (2020). Ability of selenium species to inhibit metal-induced Aβ aggregation involved in the development of Alzheimer's disease. *Analytical and Bioanalytical Chemistry*. https://doi.org/10.1007/s00216-020-02644-2

Vijayalaxmi, S., Jayalakshmi, S. K., & Sreeramulu, K. (2015). Polyphenols from different agricultural residues: Extraction, identification and their antioxidant properties. *Journal of Food Science and Technology, 52*(5), 2761–2769. https://doi.org/10.1007/S13197-014-1295-9

Wianowska, D., & Gil, M. (2019). New insights into the application of MSPD in various fields of analytical chemistry. *TrAC Trends in Analytical Chemistry, 112*, 29–51. https://doi.org/10.1016/J.TRAC.2018.12.028

Zhang, J., Melton, L. D., Adaim, A., & Skinner, M. A. (2008). Cytoprotective effects of polyphenolics on H_2O 2-induced cell death in SH-SY5Y cells in relation to their antioxidant activities. *European Food Research and Technology, 228*(1), 123–131. https://doi.org/10.1007/s00217-008-0915-x